Measurement and Prediction of Entrained-Flow Gasification Processes

A detailed mathematical model is used to predict local and effluent properties within an axisymmetric, entrained-flow gasifier. Laboratory experiments were conducted to provide local properties for four coal types from a gasifier operating at near-atmospheric pressure. Effects of selected model parameters and test variables were examined and compared with measurements in most cases. The comparison of predictions and measurements provides the first evaluation of capabilities and limitations of a comprehensive model for entrained-flow gasifiers.

B. W. Brown, L. D. Smoot, P. J. Smith, P. O. Hedman
Department of Chemical Engineering
Brigham Young University
Provo, UT 84602

Introduction

Modeling of coal reaction processes has received significant emphasis over the past decade (Smoot, 1981, 1984). Yet, model development has not reached the point where significant use is made of these computer codes in industrial process development. A recent panel of industrial and university professionals on research needs for coal utilization (Penner, 1983) emphasized the need for development of combustion models to the point where they will find application in the management and control of practical systems. While several models have been developed to predict global or one-dimensional results in entrained-flow gasifiers, few comprehensive models have been developed for predicting the local properties within these reaction chambers. None of these models has been evaluated by comparison with local data from gasifiers. Smoot (1981, 1984) has reviewed the state of development of both levels of modeling for pulverized coal flames, including combustion and gasification. The legitimacy of these models has been questioned in light of the complexity of the physical and chemical processes involved. However, over the past decade the state of the art has advanced to the point where such methods are approaching the potential for some direct applications.

The entire foundation of combustion process modeling relies heavily on comparison with experimental observations. Many studies have emphasized fundamental aspects of this problem such as coal pore diffusion, radiative properties of coals and chars, and coal structure and its relationship to reactions and particle changes during devolatilization. Still, the computational time requirements of these sophisticated predictive models demand the use of many simplifying assumptions. These assumptions are not always strongly supported by experimental data. Thus, demonstration of the validity and accuracy of model predictions is a continuing challenge. The codes are often too extensive to permit separate and complete evaluation of every component. Comparison with gross data such as outlet temperature or composition does little to improve confidence in model predictions. Comparison with mean values and space-resolved properties is a stronger test but only demonstrates applicability to the conditions of that one specific test.

It is the purpose of this paper to present measured data and predicted properties which combine to elucidate the characteristics of entrained-flow gasification. Gasification is difficult to test and model due to the high heating rates and low residence times involved, which result in very large gradients of temperature, composition, and reaction rates. Thus, a combined modeling and experimental effort is needed to provide insight into the operation of gasifiers. This paper presents experimental profile data obtained for four coal types and shows model predictions made with various assumptions. Predicted and measured results are compared and resulting insights into the reaction process are summarized. These comparisons demonstrate the current utility and limitations of a comprehensive model for application to coal gasification and they provide the first extensive model evaluation for gasification conditions. The effects of selected model parameters and test variables are also examined, and in most cases are compared with experimental data. A companion paper (Smoot and Brown, 1987) provides predictions and comparisons with measurements for effluent properties, but does not treat profile data. The emphasis there is on effects of test variables, including coal type, particle size, coal feed rate, and mixture ratio.

Local measurements within entrained-flow gasifiers are limited by the intrusive nature of water-quench probes, particularly in areas of steep concentration and temperature gradients in forward regions of the gasifier. In other regions, qualitative and to

B. W. Brown is presently with EG&G, Idaho Falls, Idaho.

some extent quantitative agreement between predictions and measurements was achieved for species mole fractions for Utah and Illinois No. 6 bituminous coals, Wyoming subbituminous coal, and North Dakota lignite coal. Quantitative agreement was weakest with the CO/CO_2 molar ratios for the Wyoming subbituminous and the Illinois No. 6 bituminous coals. Effluent carbon conversion comparisons agreed to within 2% except for the Illinois coal, where an 11% overprediction was made by the model. Model applicability was shown to be improved by use of kinetic rate data for the particular coal involved where available.

Additional computations were performed to evaluate effects of full or partial equilibrium assumption, volatiles stoichiometric coefficient, heterogeneous reaction rate coefficient, and extent of heat loss. The latter two model parameters had greater impact on predicted results than the first two parameters. Agreement with measurements of carbon conversion and gas composition was reasonable for acceptable values of all four variables. Further, effects of steam partitioning between primary and secondary streams, steam preheat temperatures, and oxygen/coal (O/C) ratio were examined. Only O/C ratio exhibited a dominant effect.

It is concluded from this evaluation for entrained-flow gasifiers that qualitative agreement can be achieved if sufficient basic data exist for determining fundamental rate parameters for the coal type of interest. Use of measurements and predictions provides useful insight into the physical and chemical processes occurring during gasification.

Mathematical Model

General characteristics

The computer model used for this work is an elliptic, axisymmetric, turbulent, pulverized coal-conversion model encompassing both combustion and entrained-flow gasification. The model assumptions and procedures have been documented in several sources (Smith et al., 1981; Fletcher, 1983; Smoot et al., 1984). It is not the purpose of this paper to enumerate the foundations or assumptions involved in this model, referred to as PCGC-2 (pulverized coal gasification and combustion, two-dimensional). Briefly, the axisymmetric code solves the governing gaseous fluid mechanics and reactions equations in an Eulerian framework. A continuing attempt is made to achieve a balance between model rigor and simplicity, with an effort to realize a common and justified level of detail in each of the model components. Improvements result from the ongoing process of postulation, evaluation, and revision. Turbulence is incorporated with a k-ϵ turbulence model for closure that has been modified following the suggestions of Melville and Bray (1979) for the presence of particles. The turbulent fluid motion affects many of the properties in the flow field. The gaseous reaction rates are assumed to be limited by molecular-scale mixing. Different gas-phase mixture fractions are defined for the local mass fraction of inlet carrier gas fuel f and the local mass fraction of gas evolved from the solid coal particles η. Transport equations are solved for each mixture fraction and its associated Favre-averaged variance about the mean. Statistical probability density functions are used to obtain mean properties of chemical composition, temperature, and other variables based on local instantaneous thermochemical equilibrium as determined from the mean and variance of the local mixture fractions.

The particle mechanics are solved by following representative individual particle trajectories in a Lagrangian frame of reference. Coal devolatilization and heterogeneous reaction rate processes are included. The transport of thermal radiation was solved with a six-flux model that included nonisotropic and multiple scattering from the particles. The comprehensive model predicts mean local properties throughout the axisymmetric flow field and effluent properties to help interpret experimental measurements and to assist in the understanding of the entrained gasification process.

The model requires values for several parameters. These include devolatilization and heterogeneous rate constants, molecular diffusivities, heat capacities, heats of formation, turbulence model constants, and others. These parameters were summarized and discussed by Smoot (1981). Depending upon the computation, approximately 30 model parameters are required; all of these parameters were obtained from independent experimental data and none was independently adjusted to improve agreement with observations. The effects of some of these model parameters on gasification predictions are examined herein. Smith (1987) has conducted a comprehensive statistical sensitivity analysis of these model parameters to elucidate which are most important to predicted results for pulverized coal combustion. Since the model and its options have been documented in other cited references, only two aspects of the model are discussed here, heat loss and heterogeneous rate constants.

Heat loss

Coal gasifiers are not adiabatic. When energy transport due to radiation and convection is included, gas properties become a function of the enthalpy as well as the mixture fractions (and hence local equivalence ratio). The gas phase energy equation couples with the entire system and results in an increase in the computational time required for a converged solution. In an attempt to account for nonadiabatic reactor performance without this computational time penalty, a simplified approximation to model reactor heat loss was used. In this method, the adiabatic gas enthalpy h_a is calculated as a conserved scalar from the inlet gas mixture fraction f and the coal gas mixture fraction η as follows:

$$h_a = h_c\eta + (1 - \eta)[h_p f + (1 - f)h_s] \tag{1}$$

where h_c is the coal enthalpy, h_p is the primary gas enthalpy, f is the mass fraction of fuel elements in carrier gas stream only, and h_s is the secondary gas enthalpy. The total amount of sensible heat, Q_t, that could be lost from the reactor is approximated by

$$Q_t = C_p(T_a - T_\infty) \tag{2}$$

where C_p is the average heat capacity, T_a is the adiabatic gas temperature, and T_∞ is the mixed temperature of the oxygen and steam feed streams. If the fraction γ of the sensible heat lost from the reactor is specified, the gas enthalpy can be approximated by

$$h_g = h_a - \gamma Q_t = h_a - \gamma C_p(T_a - T_\infty) \tag{3}$$

where h_a is calculated from Eq. 1. Thus, the local gas enthalpy is calculated as a conserved scalar from f and η when the fractional sensible heat loss factor γ is provided. The heat loss factor

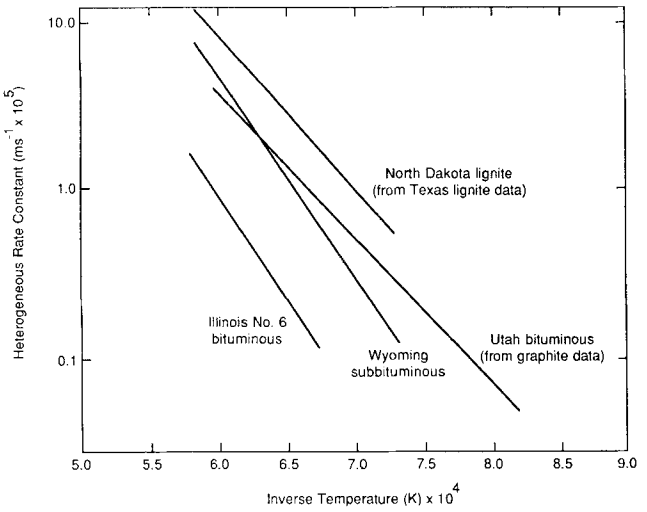

Figure 1. Arrhenius plot: experimental rate data for char-CO_2 reaction.

Data from Goetz et al. (1982), except Utah bituminous coal, from Mayers (1934) using graphite data

approach assumes that the same percentage of heat is taken from every region in the flow chamber. Particle ethalpies are still calculated from the complete particle energy equation, including radiation.

Calculations in this paper, except for parametric sensitivity computations, assumed a heat loss factor γ of 0.5. The experimental reactor was not water-cooled. Actual heat loss was estimated using three techniques: enthalpy balances on entering and exiting streams, calculation of convection and radiation from the reactor shell, and conduction through the reactor wall (Brown, 1985). The heat loss factor corresponding to these calculated values ranged from 0.45 to 0.60. The major effect of this heat loss is to lower the gas temperatures throughout the computational field. This temperature change affects the velocity field and the coal reaction rates, so that lower coal conversions are obtained.

Heterogeneous rate constants

There is a wide variability in measured heterogeneous reaction rates for various coal types. In order to obtain reliable predictions for carbon conversion rates in a gasifier, reasonable values for these rate constants are required. Figure 1 shows Arrhenius rate data used for the char-CO_2 reaction for three of the four coal types studied. No data were available for the Utah coal, and so values for graphite reaction with CO_2 (Mayers, 1934) were used. Additional work by Brown (1985) has sug-

Table 1. Selected Kinetic Parameters for Particle Model

Process	Reaction	Rate Constant	Coal Type	Ref.*	Parameters		
					Y_1^*	A_1	E_1
Devolatilization	Raw coal $\xrightarrow{k_1} Y_1$ (volatiles)$_1$ + $(1 - Y_1)$ (char) simultaneously with reaction 2	$k_1 = A_1 \exp(-E_1/RT_j)$	Utah bit.	(1)	0.39	$3.7 \times 10^5 s^{-1}$	7.36×10^8 J/kmol
			Ill. No. 6 bit.	(2)	0.31	3.7×10^5	2.08×10^8
			Wyo. subbit.	(2)	0.38	3.7×10^5	9.57×10^9
			N. Dak. lignite	(2)	0.34	2.0×10^5	2.08×10^8
					Y_2^*	A_2	E_2
	Raw coal $\xrightarrow{k_2} Y_2$ (volatiles)$_2$ + $(1 - Y_2)$ (char) simultaneously with reaction 1	$k_2 = A_2 \exp(-E_2/RT_j)$	Utah bit.	(1)	0.60	1.46×10^5	2.51×10^8
			Ill. No. 6 bit.	(2)	0.60	1.46×10^5	3.33×10^8
			Wyo. subbit.	(2)	0.60	1.46×10^5	1.32×10^8
			N. Dak. lignite	(2)	0.65	1.67×10^5	3.33×10^8
Char oxidation with O_2	$2C + O_2 \xrightarrow{k} 2CO$	$k = T_j(A + BT_j)$	Utah bit. Ill. No. 6 bit. Wyo. subbit. N. Dak. lignite	(3)	$A = -1.68 \times 10^{-2}$ ms$^{-1} \cdot$ K^{-1} $B = +1.32 \times 10^{-5}$ ms$^{-1} \cdot$ K^{-2}		
					n	A, ms$^{-1} \cdot$ K^{-1}	E, J $\cdot$ kmol^{-1}
Char oxidation with CO_2	$C + CO_2 \xrightarrow{k} 2CO$	$k = AT_j^n \exp(-E/RT_j)$	Utah bit.	(4)	1.0	4.40	1.62×10^8
			Ill. No. 6 bit.	(5)	1.0	242.	
			Wyo. subbit.	(5)	1.0	19.4	2.36×10^8
			N. Dak. lignite	(5)	1.0	12.3	1.78×10^8
							1.65×10^8
Char oxidation with H_2O	$C + H_2O \xrightarrow{k} CO + H_2$	$k = AT_j^n \exp(-E/RT_j)$	Utah bit.	(4)	1.0	1.33	1.47×10^8
			Ill. No. 6 bit.	(6)	1.0	4.26×10^4	3.16×10^8
			Wyo. subbit.	(4)	1.0	1.33	1.47×10^8
			N. Dak. lignite	(6)	1.0	208.	2.40×10^8

*(1) Ubhayaker et al. (1977). (2) Kobayashi et al. (1977). (3) Field (1969). (4) Mayers (1934). (5) Goetz et al. (1982). (6) Otto et al. (1979).
**Values were deduced from corresponding references.

gested that these rates are too high for the Utah coal. Experimental data have been limited to lower temperature regimes normally less than 1,700 K. This poses problems because the predicted peak local gasifier temperature usually exceeds 2,000 K, and the rate constants must be extrapolated beyond the temperature range of the experimental data. The parameters used in this study are summarized in Table 1. The rate constant for the char-oxygen reaction uses the linear correlation of Field (1969), which fits the data up to 2,200 K. The rate constants used for the carbon-steam reactions and the devolatilization rate constants are also shown in Table 1. Effects of the magnitude of these devolatilization and heterogeneous reaction rates were examined through a set of computations.

Experimental Method

Gasifier and test program

Figure 2 shows the construction of the laboratory-scale gasifier. The coal/oxygen flame was established by first igniting a methane/oxygen flame within the reactor through the use of a hydrogen/oxygen torch. Once the reactor had been allowed to equilibrate thermally, coal was gradually introduced into the reactor as the methane flow was decreased. The coal, oxygen, and argon tracer were premixed and injected as the primary stream at 367 K and the steam with helium tracer was injected through the annular secondary stream at 450 K. Inert gases were used for sight window purge (nitrogen), and for primary and secondary stream tracers (argon and helium).

Samples were obtained with a water-quench probe whose position could be varied radially and axially within the reactor.

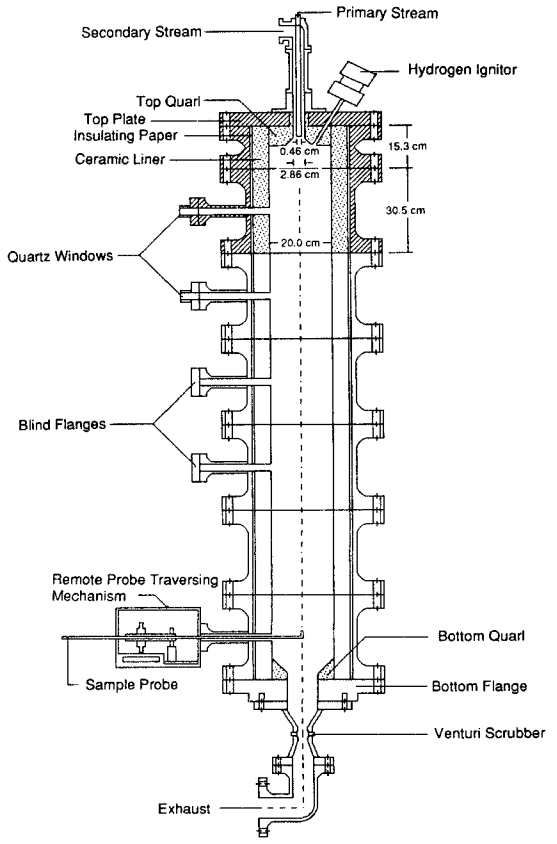

Figure 2. Laboratory-scale gasifier.

In earlier experiments (Soelberg et al., 1985), isokinetic samples were sought but these attempts were hampered by the repeated plugging of the probe pressure taps. In further testing, the use of the isokinetic probes was discontinued. Gaseous and solid char samples were separated from the quench water and analyzed with an HP-5830 gas chromatograph and a Perkin-Elmer 240 solid elemental analyzer. The quench water was analyzed for dissolved gaseous species using ion-specific electrodes (Price et al., 1983; Burkinshaw et al., 1983).

Four coal types were used in this study: Utah bituminous, Wyoming subbituminous, North Dakota lignite, and Illinois No. 6 bituminous. Coal properties, experimental operating con-

Table 2. Coal Properties, Experimental Test Conditions, and Effluent Data

	Utah Bit.	N. Dak. Lignite	Wyo. Subbit.	Ill. No. 6 Bit.
	Proximate Analysis wt. %			
Moisture	2.4	19.0	15.0	6.7
Ash	8.3	6.1	5.8	10.4
Volatiles	45.6	35.1	38.8	39.4
Fixed Carbon	43.7	39.8	40.4	43.5
High Heating Value (MJ/kg, dry)	29.8	17.9	23.7	27.4
	Elemental Analysis, dry, wt. %			
Ash	8.5	6.9	5.2	11.2
H	6.0	4.2	4.5	4.7
C	71.0	57.6	65.1	66.9
N	1.3	1.0	1.1	1.4
S	0.5	1.2	0.5	4.3
O	12.7	29.1	23.6	11.5
	Test Conditions			
Primary flow rate, kg/s	0.00729	0.00774	0.0066	0.00922
Primary comp., mol frac				
O_2	0.850	0.644	0.751	0.814
Ar	0.126	0.121	0.084	0.122
H_2O	0.024	0.235	0.165	0.064
Sec. flow rate, kg/s	0.00184	0	0	0.000666
Sec. comp. mol frac				
H_2O	1.000	—	—	1.000
Primary particle loading, kg coal/kg primary gas	0.910	1.003	0.933	0.892
Particle size dist., μm, approx. from measured dist.				
20%	3	5	4	8
20%	20	13	10	20
20%	28	32	20	40
20%	50	50	40	63
20%	80	100	100	126
Mass mean diameter as modeled	36	40	35	51
Coal heat of formation, MJ/kg	−1.20	−2.95	0.410	0.385
	Effluent Gas Properties Comp., mole %, dry, inert free			
CO	51.1	42.5	46.4	45.0
CO_2	23.6	30.5	29.6	30.2
H_2	24.7	25.8	23.4	21.9
CH_4	0.3	0.7	0.3	0.7
Cold gas effic.*	44.3	52.7	49.2	40.0
Approx. exit gas temp., K	1,350–1,400**	1,320	1,330	1,380

*HHV cooled products/HHV coal × 100
**Estimated.

ditions, and some effluent data are given in Table 2. Exit gas temperatures in Table 2 were approximated from water-gas shift equilibrium considerations. The temperature value for the Utah coal from this method was inconsistent due to high steam feed rates. However, exit temperatures for the Utah coal are thought to be similar to those for the other three coals. These values are generally consistent with inner wall thermocouple measurement near the exit of about 1,100 K, with the thermocouple bead just below the surface of the insulation. They are also similar to values reported by Coates (1984) of about 1,340 K. Experiments were performed to determine reactor operating conditions for the tests and are reported elsewhere (Brown, 1985). Oxygen-to-coal and steam-to-coal ratios were adjusted to give high values of carbon conversion and product gas heating values. For the subbituminous and lignite coals, coal moisture was used as the source of steam, and steam feed rate was not a parameter in these experiments.

Data reduction

Calculation of carbon conversion values was performed by two independent methods. In one method, coal ash was used as an inert trace constituent for the solid phase. However, elemental conversion values using the ash tracer method were subject to an error of ±14% due to the technique used for solids analysis. In a second method, argon, which was used to entrain the coal into the reactor, was also used as an inert gas tracer. From an argon balance, the effluent gas flow rate was calculated. Then from a mass balance on carbon and gas-phase composition measurements, carbon conversion was computed. The argon tracer method had an error bound of ±3.0%. Effluent gas flow rates, measured with a gas flowmeter, independently agreed with calculated values to within an average 4% with calculated values for 10 tests. Thus, the argon method was used for all experimental carbon conversion values reported herein.

The use of water-quench probes made the direct measurement of steam mole fraction impossible. Thus, a hydrogen elemental balance was used to calculate steam mole fraction (Brown, 1985). All of the hydrogen not accounted for in other chemical species was assigned to steam. The method further assumed complete radial mixing of the argon trace gas, which was not valid at the initial sampling location. A second method for calculating steam mole fraction, based on carbon and hydrogen balances, was used by Soelberg et al. (1985), and is included for the 0.13 m axial position in Figure 3 (filled symbols). This method did not assume complete gas mixing, which accounts for the large difference between the two methods. Both calculation methods use data from char ash analysis, which is subject to an error of ±14%.

Experimental and Predicted Results

Utah bituminous coal

Figure 3 shows predictions and experimental data at the reactor centerline for the Utah bituminous coal tested by Soelberg et al. (1985). The filled symbols represent data reduction methods of Soelberg et al. whereas the open symbols are for the same data treated by the data reduction methods of this study. Some agreement between the data and the prediction is noted, particularly for the CO_2 concentration. Exit concentrations are predicted within 5% and predicted effluent carbon conversion is 0.80, compared to 0.82 determined experimentally. However, significant differences exist between the calculation and the data near the reactor inlet for several of the gas species. The discrepancies in the forward regions of the reactor can be attributed to several factors. Measurements in the forward regions are

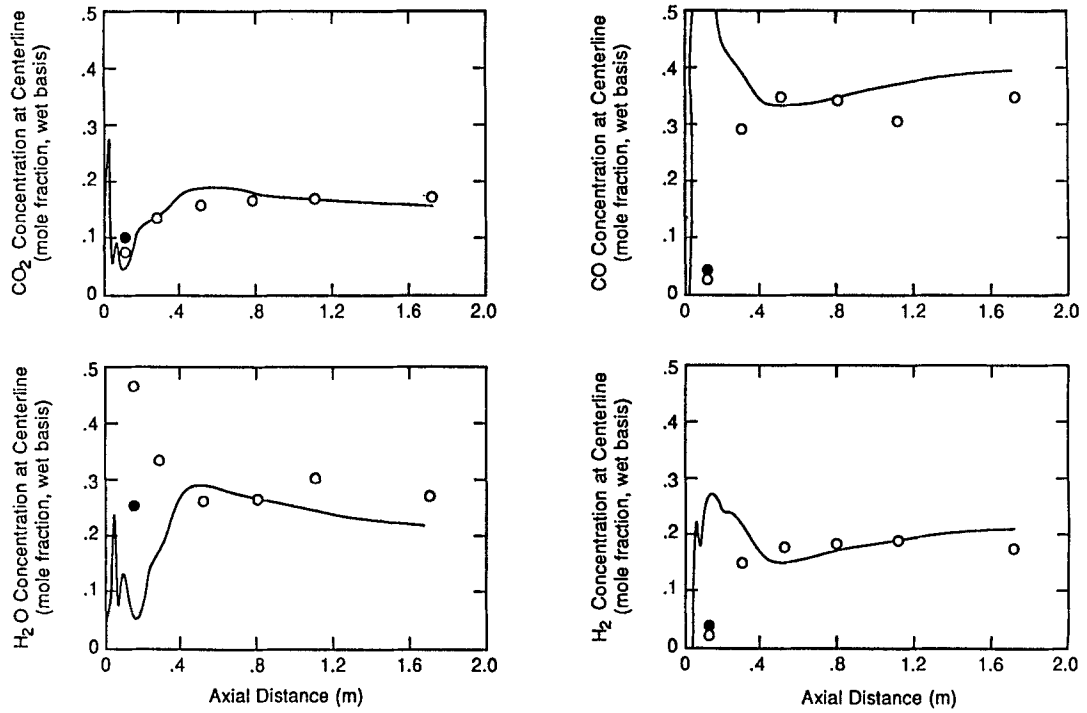

Figure 3. PCGC-2 predictions and experimental data at reactor centerline, Utah bituminous coal.

● Steam concentration calculation method of Soelberg (1985)
O This study calculation method

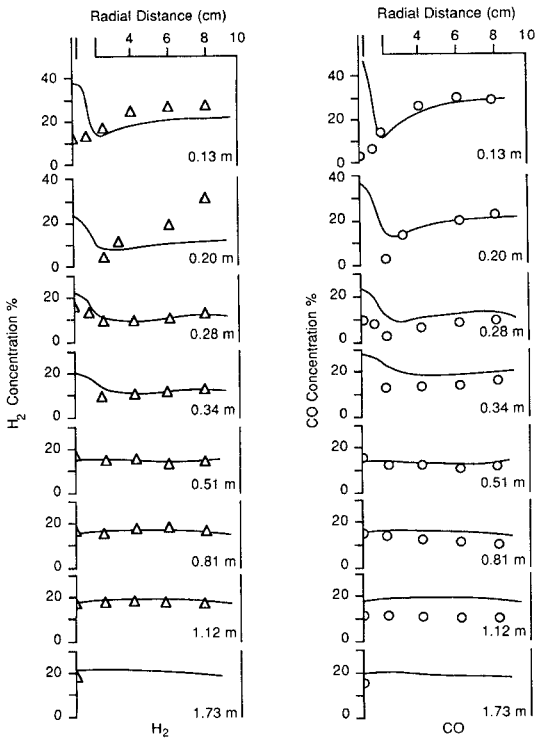

Figure 4. H_2 and CO radial profiles of predictions and experimental data, Utah bituminous coal.

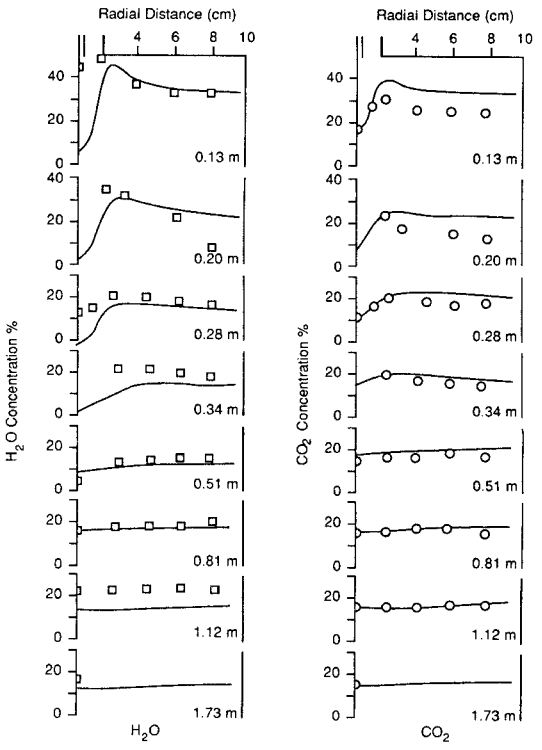

Figure 5. H_2O and CO_2 radial profiles of predictions and experimental data, Utah bituminous coal.

less accurate due to high gradients, high solids loading, plugging, and high temperatures. The experiments conducted by Soelberg et al. show evidence of such problems; hence no data are available for the centerline position at the 0.20 m axial location.

Formation of CO and H_2 is predicted to start nearer the reactor inlet than is observed experimentally, while peak values significantly higher than experimental are predicted. This discrepancy in the forward region suggests that either devolatilization rates are being inadequately modeled for the Utah coal or that onset of ignition is delayed beyond that predicted, possibly by the cold probe. The current devolatilization model assumes that elemental evolution rates (e.g., C, H, O) are proportional to overall weight loss. The Utah coal has the highest elemental carbon and hydrogen content, and the lowest oxygen content of the four coals, which would lead to high predicted CO and H_2 concentrations, compared to other coal types.

The predicted particle residence time for the Utah coal was about 340 ms. Higher coal throughputs lead to decreased particle residence times and may conceivably displace the reaction zone away from the inlet of the gasifier. Higher coal feed rates, yielding shorter residence times, were subsequently evaluated by other investigators with the Utah coal (Azuhata et al., 1986), but measurements were made only at the reactor exit; no detailed reactor profiles were obtained.

Radial profiles of major gas species are shown in Figures 4 and 5. Good qualitative agreement is observed in trends for experimental data and model predictions except in forward regions near the centerline, as discussed above. Quantitative agreement between experimental data and predictions is generally within 5 mol%, and is within 1% in many cases. The recirculation zone evident in experimental data, near the top outside wall of the reactor, is matched particularly well for the CO and H_2O gas species. Predicted trends in the H_2 and CO_2 species agree qualitatively with those exhibited by the data. Agreement between data and predictions is poor at the 0.20 m position. This may be due partly to experimental difficulties, however, since the data shown are inconsistent with profiles at other axial positions. Downstream of the 0.51 m position, data and predicted profiles are essentially flat, with qualitative agreement between data and predictions for most of the axial positions.

Wyoming subbituminous coal

Predictions and experimental data at the reactor centerline for the Wyoming subbituminous coal are shown in Figure 6. Predicted hydrogen concentration shows good agreement with experimental data. Predicted H_2O mole fraction also shows quantitative agreement with values calculated from measured data, near the reactor exit. The data from repeat experiments (represented by filled symbols and obtained under more controlled conditions), show a forward region of low H_2O concentration followed by an increase in concentration at about 0.50 m and then a slight decrease in concentration toward the reactor exit. This suggested tendency (only three data points) is also predicted by the model. The rapid decrease in predicted H_2O concentration between the 0.05 m and 0.20 m position is due to two factors: dilution by the evolution of other gas species (H_2 and CO), and the heterogeneous reaction with char consuming the steam (heterogeneous char reaction also being evidenced by the decrease in CO_2 concentration at this same axial position). An increase in steam concentration near 0.40 m is possibly due to the water-gas shift reaction producing H_2O. At positions below 0.60 m, the shift equilibrium is presumably favoring H_2,

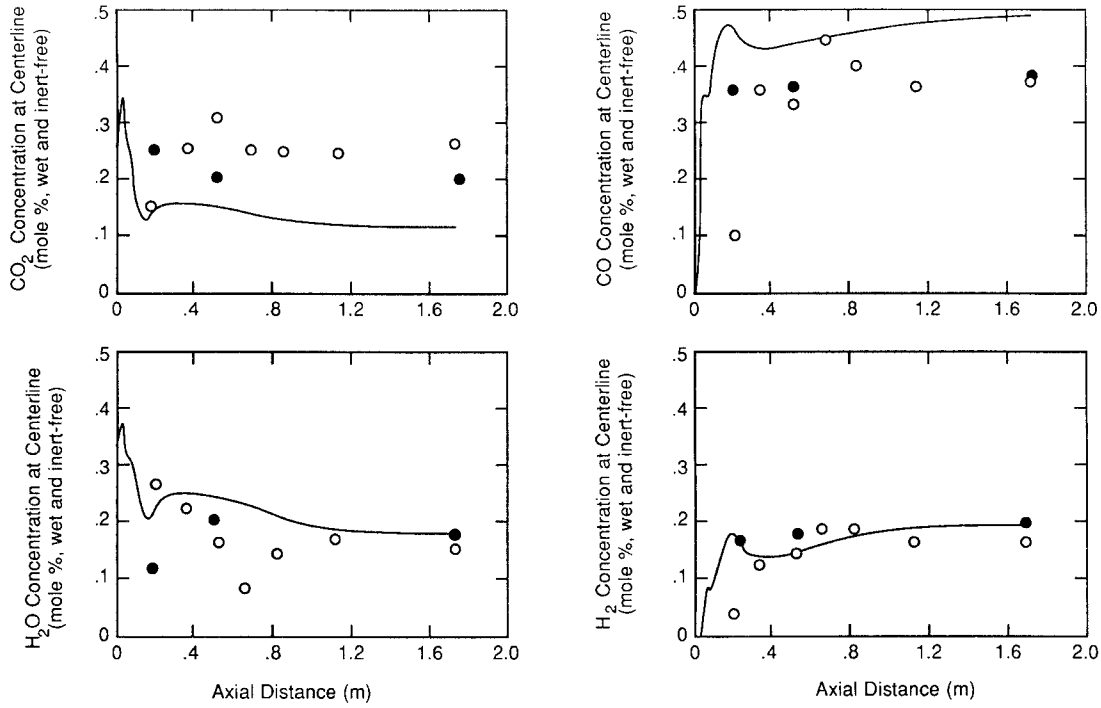

Figure 6. PCGC-2 predictions and experimental data at reactor centerline, Wyoming subbituminous coal.
● Repeat experiments

and slow heterogeneous reaction with char also leads to decreased H_2O concentration.

Experimental data for carbon monoxide and carbon dioxide gas concentrations are not as well matched by the model predictions as data for the hydrogen-containing species. Experimental data show that these species concentrations change only a few percent after the initial sampling position (0.21 m). This trend is predicted by the model, but the predicted CO/CO_2 ratio is much higher than the measured ratio at the reactor centerline. Carbon conversion at the reactor exit of 0.92 is matched by a predicted value of 0.92. Average particle residence time is predicted to be about 270 msec.

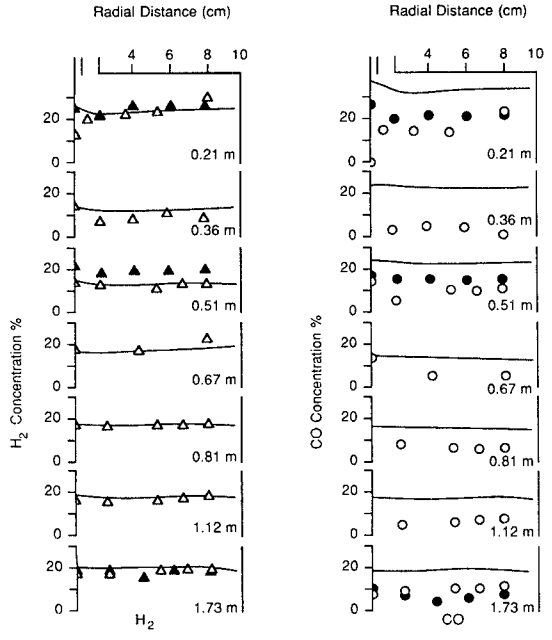

Figure 7. H_2 and CO radial profiles of predictions and experimental data, Wyoming subbituminous coal.
● Repeat experiments

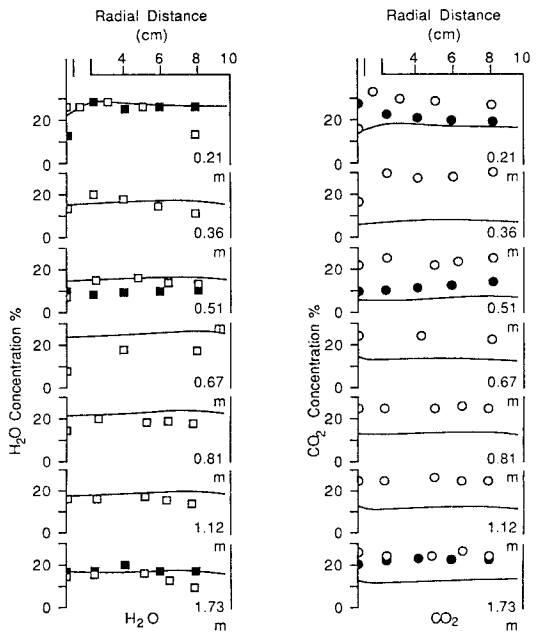

Figure 8. H_2O and CO_2 radial profiles of predictions and experimental data, Wyoming subbituminous coal.
● Repeat experiments

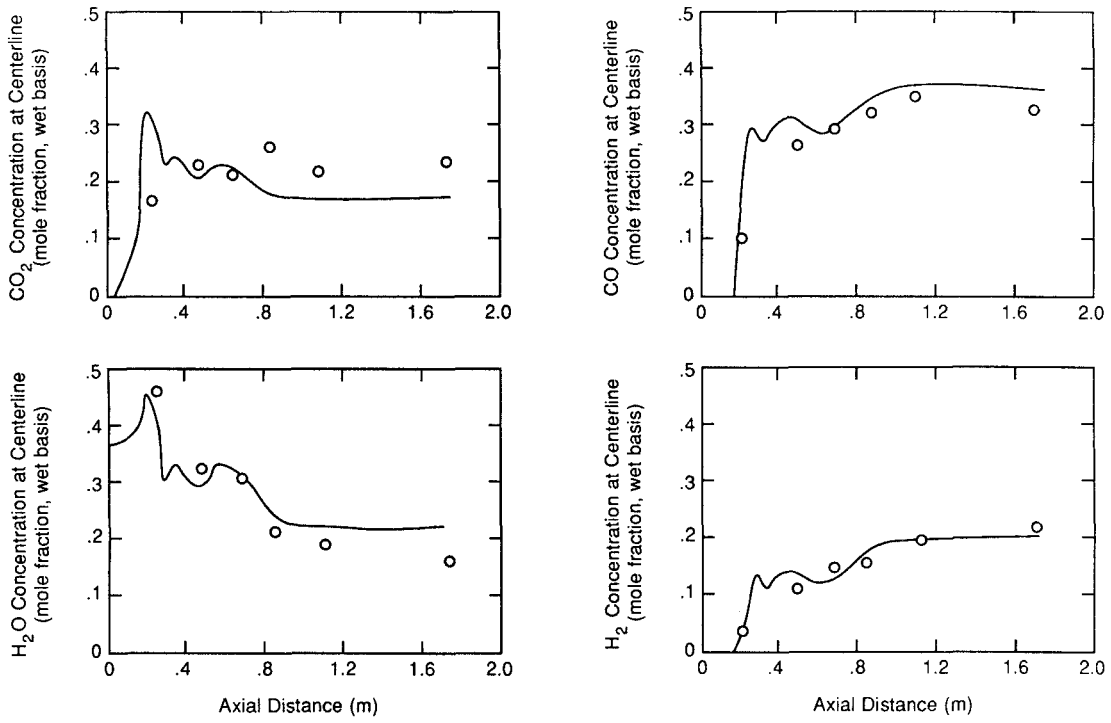

Figure 9. PCGC-2 predictions and experimental data at reactor centerline, North Dakota lignite coal.

Constant operating conditions were difficult to maintain during experiments with the Wyoming subbituminous coal, and this may have contributed to differences in measured and predicted CO/CO_2 ratio. Coal feed rate was subject to higher variability, and coal moisture varied among the different barrels of coal by up to 6%. CO and CO_2 concentrations are very sensitive to input stoichiometry (O_2:H_2O:C ratio), which is determined by coal feed rate and moisture content. The average stoichiometry was used for model predictions for all of the experiments with the Wyoming coal. If the coal feed rate during a given experiment was lower than that used by the model, the predicted CO concentrations would be lower, CO_2 concentrations would be higher, and better agreement with the experimental data would be achieved.

Figures 7 and 8 show radial profiles of data and predictions. The predicted profiles are essentially flat, except for slight gra-

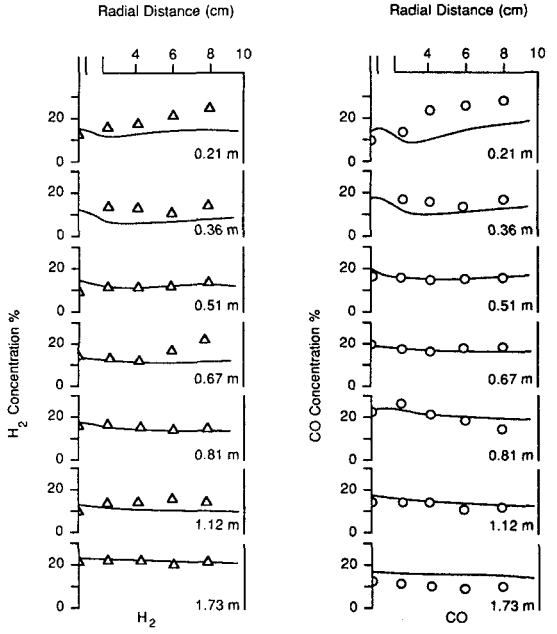

Figure 10. H_2 and CO radial profiles of predictions and experimental data, North Dakota lignite coal.

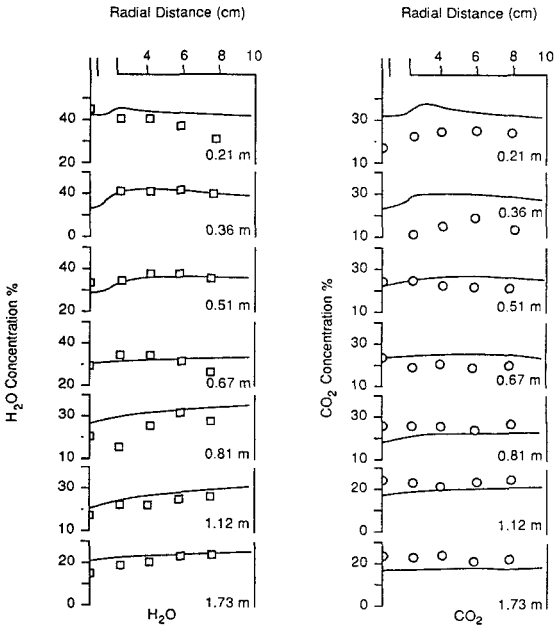

Figure 11. H_2O and CO_2 radial profiles of predictions and experimental data, North Dakota lignite coal.

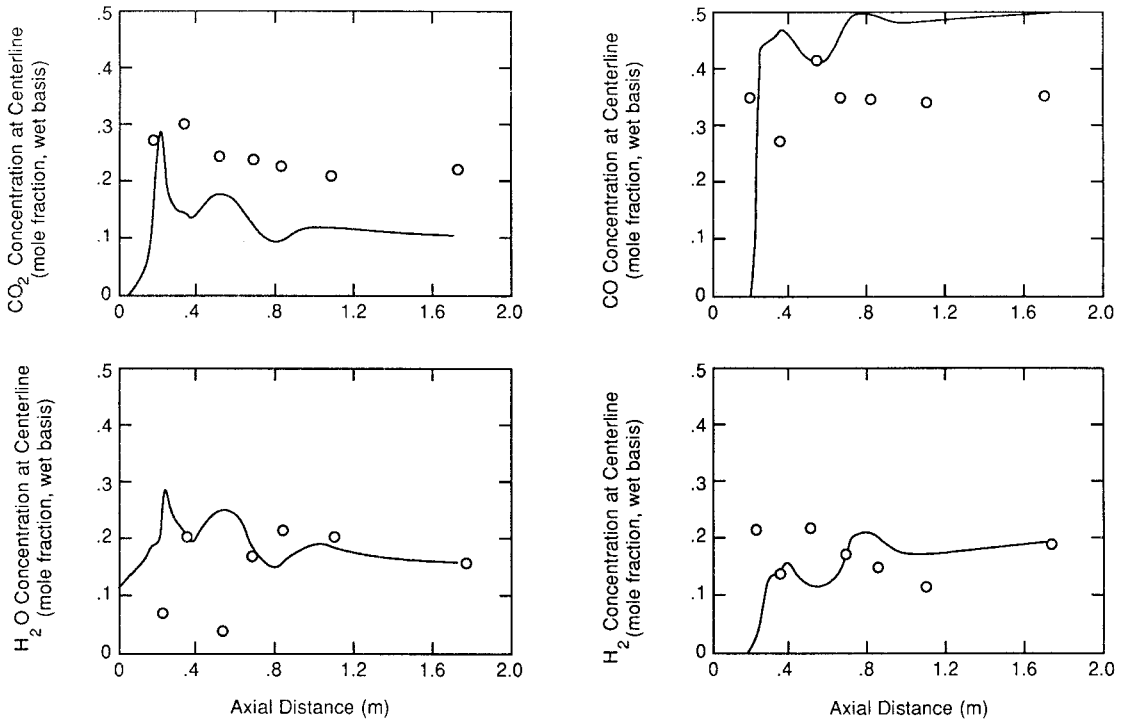

Figure 12. PCGC-2 predictions and experimental data at reactor centerline, Illinois No. 6 bituminuous coal.

dients near the reactor inlet. As with the axial profiles, hydrogen shows the best agreement between experimental data and model predictions. Predicted H_2O mole fractions are also in relatively good agreement with the radial data profiles. Data at the 0.67 m position are not as well matched due to a fouled probe, which resulted in low sampling rates (samples were taken at only three radial locations). Char compositions, used to calculate H_2O mole fractions, were affected by the sampling problems.

Predicted CO and CO_2 radial profiles vary substantially from the measured values. The data trends, the flat profiles in Figures 7 and 8, are modeled correctly, but the CO/CO_2 ratio is predicted to be much higher than that observed. The repeat experiments (filled symbols), in which the coal feed rate was more con-

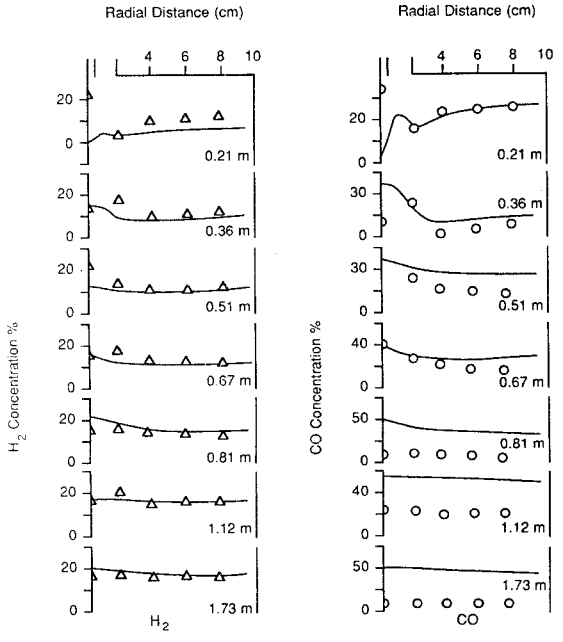

Figure 13. H_2 and CO radial profiles of predictions and experimental data, Illinois No. 6 bituminous coal.

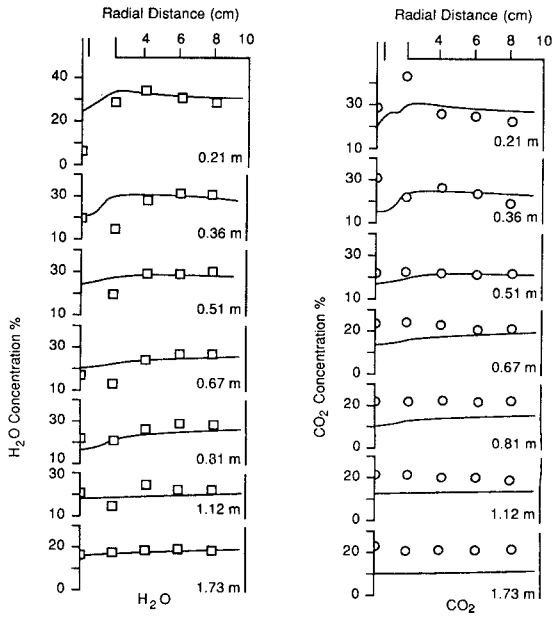

Figure 14. H_2O and CO_2 radial profiles of predictions and experimental data, Illinois No. 6 bituminous coal.

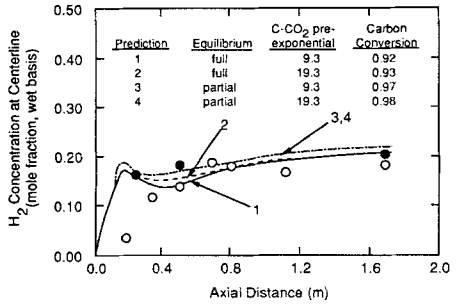

Figure 15. Effect of equilibria and C-CO_2 preexponential rate constant on predictions, Wyoming subbituminous coal.

O Initial experiments; ● repeat experiments

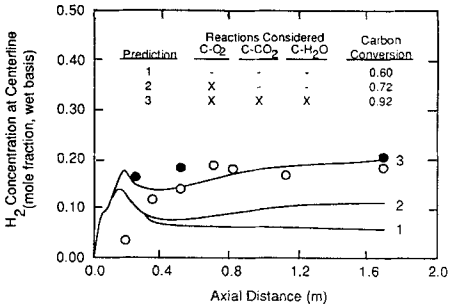

Figure 17. Effect of including various reactions on H_2 concentration and carbon conversion predictions, Wyoming subbituminous coal.

Input conditions given in Tables 1, 2
O Initial experiments; ● repeat experiments

trolled, generally showed better agreement between predictions and data than did the initial experiments.

North Dakota lignite

Figure 9 shows centerline data and predictions for the North Dakota lignite coal. Trends exhibited by the data are matched well by model predictions and quantitative agreement with the model is achieved for most of the experimental locations. The devolatilization region (initial formation of gas species) is described the best among the four coals investigated, indicated by quantitative agreement of the model predictions with data at the initial sampling position. Predicted carbon monoxide, hydrogen, and steam mole fractions agree with the experimental data, with the axial profile trends in very good agreement. Predicted CO_2 concentrations also show good agreement with measured values in the top 0.80 m of the reactor.

Radial profiles in Figures 10 and 11 also show good agreement between experimental data and model predictions for almost every axial position. Measured trends in gas composition in the recirculation zone (near the top outside wall of the reactor) also agree with those predicted, except for CO_2. Agreement between data and model predictions for CO_2 concentrations improve at lower axial positions in the reactor. Experimental conversion at the reactor exit of 0.81 agrees with the predicted value of 0.81. Average particle residence time is predicted to be about 320 msec.

Illinois No. 6 bituminous coal

Centerline experimental data and PCGC-2 predictions for the Illinois No. 6 bituminous coal are seen in Figure 12. The agreement is not as good at the reactor centerline as that shown by the other coal types. H_2O concentrations at the 0.21 m and 0.51 m axial positions are much lower than the other axial values. This is possibly due to the same reasons mentioned for the H_2O concentrations for the Utah coal, which was the only other coal tested that used steam injected in the secondary stream. The low H_2O fraction makes the other gas species relatively high (on a wet basis), accounting for some of the discrepancy between the prediction and the experimental data at the 0.21 and 0.51 m positions. The predicted CO/CO_2 ratio is much higher than the experimental values, primarily due to the higher predicted conversion of 0.90, compared to 0.81 for the experimental value. For a fixed amount of oxygen, a larger amount of carbon in the gas phase will increase the CO/CO_2 ratio. Average particle residence time is predicted to be 190 msec.

Another reason for the difference between predicted and experimental conversion values is the bimodal particle size distribution for the Illinois coal. The distribution, as input to the model, could not adequately describe the observed size distribution, particularly the preponderance of particles larger than 100 μm. Larger particles were predicted to react to a much lesser degree. Inclusion of larger particles in the size distribution could decrease overall conversion by 5–10% (Brown, 1985).

Radial profiles of experimental data and predictions are seen in Figures 13 and 14. Trends exhibited by the data are matched

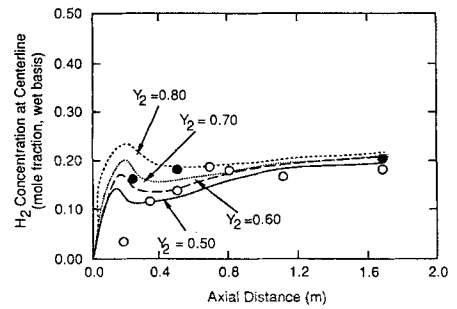

Figure 16. Effect of volatiles stoichiometric coefficient Y_2 on predictions, Wyoming subbituminous coal.

Full equilibrium; O initial experiments; ● repeat experiments

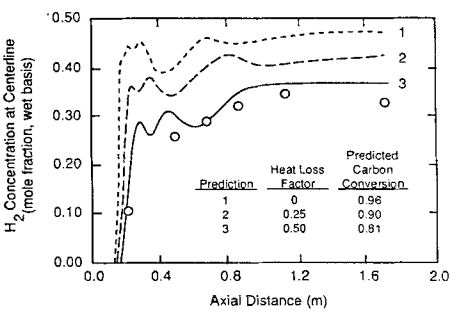

Figure 18. Effect of heat loss on carbon conversion and CO concentration at reactor centerline, North Dakota lignite coal.

O Experimental data

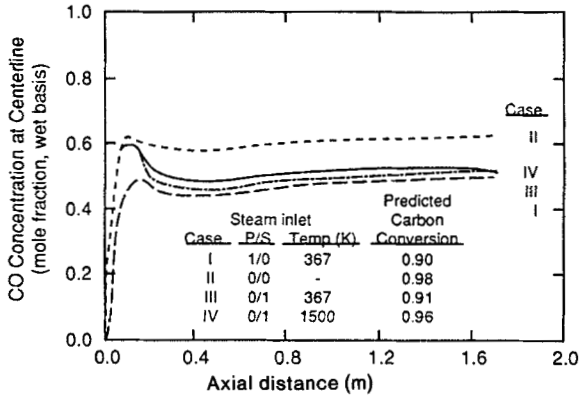

Figure 19. Predicted effects of steam partitioning and steam preheat temperature at reactor centerline, Wyoming subbituminous coal.
Input conditions given in Tables 1, 2

quite well by the model, particularly for values off the centerline. Quantitative agreement is very good for all gas species at axial positions close to the burner. As time (and axial position) progresses, the predicted CO/CO_2 ratio diverges from that measured experimentally.

For the Illinois coal, as with the Utah coal, the observed gas concentrations in the forward regions near the centerline differ greatly from predicted values. However, the data suggest a more rapid coal reaction process than observed for the Illinois coal, with product gas concentrations much higher than predicted in this forward, near-centerline region. Somehow this early mixing-reaction process is very sensitive to some model parameters, because predictions for the two bituminous coals differ so dramatically, and neither agrees with observations.

The Illinois coal prediction used a higher coal moisture content and higher inlet velocity than the prediction for the Utah coal. Both of these parameters delay the onset of ignition for the Illinois coal prediction compared to that for the Utah coal, as seen in Figures 3 and 12.

Parameter Sensitivity Analysis

A sensitivity analysis of several model parameters related to gasifiction has been conducted. In most cases, results are compared with measured data. An independent sensitivity analysis for combustion applications has been reported by Smith (1987). Two types of variables were included in this analysis, model parameters and test variables.

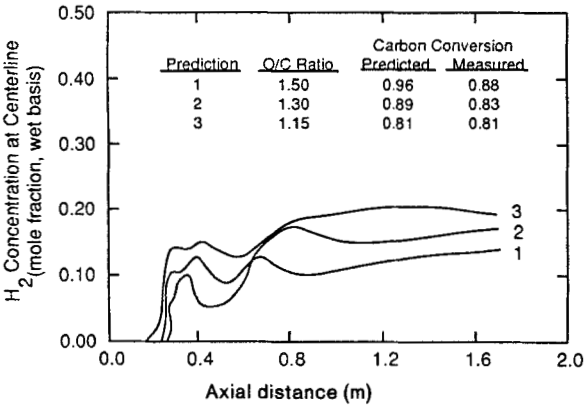

Figure 20. Predicted effects of O/C ratio on H_2 concentration and carbon conversion, North Dakota lignite.

Effects of model parameters

Several model parameters were varied to determine their influence on the gasification process. The parameters investigated were full/partial equilibrium, coal volatiles stoichiometric coefficients, heterogeneous reaction rates, and heat loss factor.

Gas phase chemistry in the model can be treated as being in full equilibrium at a specified temperature, or in "partial" equilibrium wherein fuel-rich mixtures are not allowed to oxidize fully (Fletcher, 1983). In these computations, coal offgas formation was limited to CO, C_2H_2, C_2H_4, and N_2 (dictated by elemental balances) in fuel-rich regions of the gasifier. Oxidized species, such as CO_2 and H_2O, were not allowed to form. In regions of the gasifier with equivalence ratios less than 2.0, full equilibrium was assumed. Figure 15 shows the effects of full and partial equilibrium on calculations with Wyoming subbituminous coal. Differences between the two cases are small. The full equilibrium model gave slightly better agreement, by up to 6%, with measured data for carbon conversion (0.92) and hydrogen concentration (shown), as well as temperature and carbon oxides concentration (not shown), but these differences are not statistically significant.

Coal volatiles stoichiometry is important in gasification because most of the coal mass loss occurs through this process and because coal not devolatilized is heterogeneously oxidized by much slower processes than occur by coal devolatilization and subsequent gas phase oxidation of volatile matter. Figure 16 shows experimental data for Wyoming subbituminous coal and predictions with the coal volatile matter coefficient (Y_2 in Table 1) set at 0.5, 0.6, 0.7, and 0.8. This coefficient sets an upper limit on the fraction of coal that can be devolatilized. Effects of such a significant change in volatiles stoichiometry were less dramatic than anticipated. Exit hydrogen concentration varied by only about 2%, with intermediate values for hydrogen concentration varying by only 10% among the different predictive cases. Carbon conversion at the reactor exit varied from 90 to 96%, and exit CO concentration (not shown) was essentially the same for all four predictions. Analyses of these predictive results indicates that use of lower values for the maximum coal volatiles fraction Y_2 allows feed oxygen not otherwise consumed by the volatile matter oxidation to rapidly oxidize the remaining char particle, resulting in a carbon conversion level similar to that predicted when higher values of Y_2 were assumed.

Devolatilization of coal and heterogeneous reactions of char with oxygen, carbon dioxide, and steam are competing reaction processes treated in the model. Calculations were performed to investigate the relative importance of heterogeneous reaction rates of char with O_2, CO_2, and H_2O, Figure 17. With Y_2 volatiles fraction of 0.6 and no heterogeneous reaction, carbon conversion was 60%, as expected. Allowing the $C\text{-}O_2$ reaction to occur simultaneously resulted in a carbon conversion value of 72%, while including the $C\text{-}CO_2$ and $C\text{-}H_2O$ reactions increased carbon conversion to 92% and provided the best agreement with measured hydrogen concentration (measured to be 92% experimentally). Thus, all of the heterogeneous reactions appear to be important in the predicted results.

Heat loss from the reactor can be modeled with a constant

heat loss factor, Eq. 3, or through formal solution of the energy equation. The former method, described above, provides a numerically efficient way to evaluate effects of heat loss. Figure 18 shows predicted and experimental carbon monoxide concentration for North Dakota lignite coal for heat loss factor values of 0, 0.25, and 0.50. Correlation with experimental data was much better using a value for heat loss factor of 0.5 (equivalent to about 28% heat loss experimentally), as was carbon conversion and other permanent gases (not shown).

Effects of test variables

Predictions were also made for test variables related to experiments. Effects of dividing the feed steam in different proportions between the primary and secondary streams were predicted, as were effects of variation in steam inlet temperature and oxygen/coal ratio.

Partitioning of steam between the primary and secondary inlet streams in different proportions was investigated through model predictions. Figure 19 shows CO concentration and carbon conversion for four cases: steam in primary, no steam at all, steam in secondary, and much higher temperature steam in secondary. Carbon monoxide and carbon conversion are highest in the absence of steam. Model calculations coincided with trends exhibited by experiments, namely lower carbon conversion and lower CO/CO_2 ratio with increasing feed steam input in either the primary or secondary stream. However, neither steam feed location nor substantial increase in steam feed temperature had much effect on predicted gas concentration.

Oxygen-to-carbon ratio was also investigated using the theoretical model; the results for North Dakota lignite coal are shown in Figure 20. As experiments had shown, higher O/C ratio led to substantially decreased hydrogen concentration and higher carbon conversion.

Acknowledgment

The work reported in this paper was funded by the United States Dept. of Energy, Morgantown Energy Technology Center, under the direction of Holmes Webb, Gary Friggens, and Leland Paulson, and by Brigham Young University. The authors also acknowledge the work of Lynda Richmond and Linda Ward in preparation of the manuscript and figures.

Literature Cited

Azuhata, S., P. O. Hedman, and L. D. Smoot, "Carbon Conversion in an Atmospheric Entrained Coal Gasifier," *Fuel*, **65**, 212 (1986).

Burkinshaw, J. R., L. D. Smoot, P. O. Hedman, and A. U. Blackham, "Analysis of Three-Phase Sulfur and Nitrogen Pollutants in Coal Combustion Effluents," *Ind. Eng. Chem. Fundam.*, **22**, 292 (1983).

Brown, B. W., "Effect of Coal Type on Entrained Gasification," Ph.D. Diss., Chem. Eng., Brigham Young Univ., Provo, UT (1985).

Coates, R. L., personal communication, Mountain Fuel Resources Co., Salt Lake City, UT (1984).

Field, M. A., "Rate of Combustion of Size-graded Fractions of Char from a Low-rank Coal between 1,200 and 2,000 K," *Comb. Flame*, **21**, 237 (1969).

Fletcher, T. H., "A Two-Dimensional Model for Pulverized Coal Gasification and Combustion," Ph.D. Diss., Chem. Eng., Brigham Young Univ., Provo, UT (1983).

Goetz, G. J., N. Y. Nsakala, R. L. Patel, and T. C. Lao, "Combustion and Gasification Characteristics of Chars from Four Commercially Significant Coals of Different Rank," Combustion Engineering, Inc., Windsor, CT (1982).

Kobayashi, H., J. B. Howard, and A. F. Sarofim, "Coal Devolatilization at High Temperatures," *16th Symp. (Int.) Combust.*, Combustion Inst., Pittsburgh, 411 (1977).

Mayers, A. M., "The Rate of Reduction of Carbon Dioxide by Graphite," *Am. Chem. Soc. J.*, **56**, 70 (Jan., 1934).

Melville, E. K., and K. N. C. Bray, "A Model of the Two-Phase Turbulent Jet," *Int. J. Heat Mass Trans.*, **22**, 647 (1979).

Otto, K., L. Batosiewicz, and M. Shelef, "Catalysis of Carbon-Steam Gasification by Ash Components from Two Lignites, *Fuel*, **58**, (1979).

Penner, S. S., "Assessment of Research Needs of Coal Utilization to U.S. Department of Energy," Univ. Calif. Energy Center, San Diego (Aug., 1983).

Price, T. P., P. O. Hedman, and L. D. Smoot, "Measurement of Nitrogen and Sulfur Pollutants in an Entrained-Coal Gasifier," *Ind. Eng. Chem. Fundam.*, **22**, 110 (1983).

Smith, J. D., "Foundations of a Three-Dimensional Model for Predicting Coal Combustion Characteristics in Industrial Power Generation Plants," Ph.D. Diss. Chem. Eng., Brigham Young Univ., Provo, UT (in process, 1987).

Smith, P. J., T. H. Fletcher, and L. D. Smoot, "Model for Pulverized Coal-Fired Reactors," *18th Symp. (Int.) Combust.*, Combustion Inst., Pittsburgh, 1285 (1981).

Smoot, L. D. "Pulverized Coal Diffusion Flames: A Perspective Through Modeling," *18th Symp. (Int.) Combust.*, Combustion Inst., Pittsburgh, 1185 (1981).

———, "Modeling of Coal Combustion Processes," *Prog. Energy Comb. Sci.*, **10**, 229 (1984).

Smoot, L. D., and B. W. Brown, "Controlling Mechanisms for Gasification of Pulverized Coal," *Fuel*, **66**, 1249 (1987).

Smoot, L. D., P. O. Hedman, and P. J. Smith, "Pulverized Coal Combustion Research at Brigham Young University," *Prog. Energy Comb. Sci.*, **10**(2), 359 (1984).

Soelberg, N. R., L. D. Smoot, and P. O. Hedman, "Mixing and Reaction Processes in an Entrained Coal Gasifier from Local Measurements. 1," *Fuel*, **64**, 776 (1985).

Ubhayaker, S. K., D. B. Stickler, C. W. von Rosenberg, and R. E. Gannon, "Rapid Devolatilization of Pulverized Coal in Hot Combustion Gas," *16th Symp. (Int.) Combust.*, Combustion Inst., Pittsburgh, 427 (1977).

Manuscript received Jan. 16, 1986 and revision received Sept. 15, 1987.